ARTICLE IN PRESS

Available online at www.sciencedirect.com
SCIENCE DIRECT®

Nuclear Instruments and Methods in Physics Research B xxx (2006) xxx–xxx

NIM B
Beam Interactions with Materials & Atoms

www.elsevier.com/locate/nimb

Positronium ionization by short UV laser pulses: Splitting of the ATI peaks by Rabi oscillations

V.D. Rodríguez *

Departamento de Física, FCEyN, Universidad de Buenos Aires, 1428 Buenos Aires, Argentina

Available online

Abstract

The interaction between positronium and a short laser pulse is studied in the case, where the photon energy is resonant with the $1s \rightarrow 2p$ transition energy. Results from a full numerical solution of the time-dependent Schrödinger equation, and also from a variational approach based on the Coulomb–Volkov wave function to describe the final states are presented. For the initial state, a solution of the time-dependent Schrödinger equation involving the two resonantly bound states is used. This wave function exhibits Rabi oscillations as the laser amplitude increases. Using the rotating wave approximation the contribution from N-photon and $(N-1)$-photon ionization from ground and excited state with split energy levels can be identified. The theory predicts each above threshold ionization primary peak split in two peaks separated by half an appropriate Rabi frequency. It is suggested that this phenomenon could be experimentally measured by the Aarhus group working on positronium in laser fields.

PACS: 32.80.Rm; 36.10.Dr; 32.80.−t; 36.10.−k

Keywords: Positronium; Ionization; Laser pulse; Rabi oscillations

1. Introduction

Positron physics under laser fields is closely related to hydrogen under scaled intensity and frequency laser fields by using well stated scaling rules [1]. This is particularly true when the positronium life time against annihilation is longer than the laser length. Available femtosecond laser pulses (10^{-15} s) are short enough to interact with both triplet and singlet positronium decaying through 2-photon and 3-photon emission with decay times of $\tau_{\text{trip}} \sim 1.4 \times 10^{-7}$ s and $\tau_{\text{sing}} \sim 1.25 \times 10^{-10}$ s, respectively [2]. From the scaling prescription, we can verify important advantages of positronium as compared to hydrogen target. Some of the relative advantages have been cited by the Aarhus group [3] such as the larger cross sections for a given N-photon ionization process scaling as 2^{3N+1} for positronium as compared with hydrogen. Moreover, resonant enhancement multiphoton ionization REMPI experiments are better achievable with positronium targets. For instance, resonant $1s \rightarrow 2p$ excitation require $\omega = 0.1875$ a.u. ($\lambda = 243.2$ nm), which is half the frequency required by hydrogen. This frequency is within the laser frequency range of the laser to be used in coming experiments involving Ps multiphoton ionization [3,4].

Previous experimental studies on laser positronium interaction were mostly concerned with laser excitation [4,5]. On theoretical side, ab initio calculations of positronium breakup by 2–6 photon absorption from strong subpicosecond laser pulses have been published [6]. More recently, work have been addressed to considering positronium under intense laser fields accounting for laser magnetic fields effects [7].

Here, we present theoretical results employing a particular variant of our modified Coulomb–Volkov approximation MCV2$^-$ [8] to the description of above threshold ionization (ATI) of positronium. Different from the perturbative case discussed in [8], we focus on the case where the laser field is in resonance with the $1s \rightarrow 2p$ transition. Increasing laser intensity and length pulse are analyzed. The theoretical frame from [8] is used, namely a variational

* Tel.: +54 11 45763353; fax: +54 11 45763357.
E-mail address: vladimir@df.uba.ar

0168-583X/$ - see front matter © 2006 Elsevier B.V. All rights reserved.
doi:10.1016/j.nimb.2006.01.045

approach with Coulomb–Volkov states as the final trial wave function is employed. However, for the initial trial function, the bound state wave function obtained by solving the time-dependent Schrödinger for two resonantly coupled states is considered. This wave function exhibits Rabi oscillations and energy splitting. For the intermediate laser intensities our new results are compared with previous exact solutions of the time-dependent Schrödinger equation TDSE as well as with perturbative MCV2$^-$ theory [8].

Multiphoton splitting of hydrogen ATI peaks due to resonant intermediate state population have been previously found either with a perturbative analytical procedure for long laser pulses [9], or by solving the time-dependent Schrödinger equation TDSE [10].

Our purpose is to bring some light on the mechanism of this phenomenon by using a quasi-analytical theory. In this way, it is expected to complement full numerical treatments involving intensive calculations [11] that sometimes may hide the essential physics of the problem. Further, as mentioned above, this work is timely as positronium experiments are planned within the frequency and laser intensities investigated here. Likewise, the analysis of future experiments are in need of adapted theoretical approximations that are able to provide simple reliable predictions of ionization by short UV laser pulses.

In Section 2, the relevant scaling rule relating the positronium case to the hydrogen one is presented. The new theory CV-TS (Coulomb–Volkov two-states) is derived using the same variational principle for the transition amplitude employed to derive MCV2$^-$ theory [8]. For the resonant $1s \rightarrow 2p_0$ transition, the previous perturbative procedure for the initial state description is reformulated in terms of the numerically solved two-state problem. Then, the non-perturbative condition due to the resonant coupling of both states may be accounted for. In Section 3, the CV-TS is applied for pulse length within the femtosecond regime (40–80 laser cycles). The failure of the previous perturbative treatment when applied to the resonant intermediate state is illustrated by comparing with full TDSE results. The CV-TS theory improves the MCV2$^-$ in an important quantitative and qualitative ways. Rabi oscillations are displayed by solving the time-dependent Schrödinger equation for two-state problem coupled by a short laser pulse. As is expected, Rabi frequency increases with amplitude. Finally, the ATI peaks splitting in two secondary peaks for different laser intensities are shown. An explanation for this behavior is given by using the simple structure of the theory. Conclusions are drawn in Section 4.

Atomic units are used throughout unless otherwise stated.

2. Theory

2.1. Scaling

Here, the problem of positronium under a laser field and that of hydrogen are related [1]. Both cases have null total charge, thus their centers of mass CM evolve freely. The relative coordinate $\vec{r} = \vec{r_2} - \vec{r_1}$ do satisfy the following equation:

$$i\frac{\partial \Psi(\vec{r},t)}{\partial t} = \left[-\frac{\nabla^2}{2\mu} - \frac{1}{r} - q_r \vec{r}\cdot\vec{F}(\omega,t)\right]\Psi(\vec{r},t), \tag{1}$$

where the reduced mass is $\mu = m_1 m_2/(m_1+m_2)$, and the reduced charge is $q_r = (q_1 m_2 - q_2 m_1)/(m_1+m_2)$. It is noted that isotopic effects could arise from the charge for non-neutral ionic species in addition to accelerated motion of the CM [12]. Owing to the large value of the proton to electron mass ratio then $q_r \cong -1$ and $\mu \cong 1$ for hydrogen. For the positronium case, $q_r = -1$ and $\mu = 1/2$. By scaling length and time as $r_s = \mu r$ and $t_s = \mu t$ the following equation is obtained:

$$i\frac{\partial \Psi(\vec{r}_s,t_s)}{\partial t_s} = \left[-\frac{\nabla^2_{r_s}}{2} - \frac{1}{r_s} + \vec{r}_s\cdot\vec{F}_s(\omega_s,t_s)\right]\Psi(\vec{r}_s,t_s) \tag{2}$$

which describes a hydrogen atom subject to the field of scaled amplitude $\vec{F}_s(\omega_s,t_s) = \mu^{-2}\vec{F}(\omega,t)$, and frequency $\omega_s = \mu^{-1}\omega$. In short, positronium is affected by a double frequency, quadruple field amplitude and half the pulse length as compared with hydrogen. Further differences arise from the fact that relative energy is shared equally by the emitted electron and the positron flying away when measured in the laboratory system.

2.2. Coulomb–Volkov two-states variational theory

Once the positronium problem has been scaled to the hydrogen one, the ionization of hydrogen atom by an external laser radiation with electric field $\vec{F}(\vec{r},t)$ is then considered. Under non-relativistic conditions and within the electric dipole approximation, the electron wave function $\Psi(\vec{r},t)$ satisfies the time-dependent Schrödinger equation

$$\begin{aligned} i\frac{\partial \Psi(\vec{r},t)}{\partial t} &= \left[H_a + \vec{r}\cdot\vec{F}(t)\right]\Psi(\vec{r},t), \\ H_a &= -\frac{\nabla^2}{2} - \frac{1}{r}, \end{aligned} \tag{3}$$

where $\vec{r}$ is the position of the electron with respect to the nucleus identified with the center-of-mass, $\vec{F}(t)$ is the laser field in the volume of the atom and H_a is the atomic Hamiltonian. In the ionization process, the initial bound state $\phi_i(\vec{r},t)$ and the final continuum state $\phi_f^-(\vec{r},t)$ may be written as

$$\begin{aligned} \phi_i(\vec{r},t) &= \varphi_i(\vec{r})\exp(-i\varepsilon_i t), \\ \phi_f^-(\vec{r},t) &= \varphi_f^-(\vec{r})\exp(-i\varepsilon_f t), \end{aligned} \tag{4}$$

where $\varphi_i(\vec{r})$ and $\varphi_f^-(\vec{r})$ are eigenstates of the field-free Hamiltonian H_a and $\varphi_f^-(\vec{r})$ is the ingoing continuum state of momentum $\vec{k}$ normalized to $\delta(\vec{k}-\vec{k}')$. In the present section, we focus on the hydrogen atom. The scaling rules will be employed in Section 3 to apply the theory for positronium ionization by laser pulses.

The finite pulse duration is featured by a sine-square envelope. Thus, in the vicinity of the atom, the external electric field reads

$$\begin{cases} \vec{F}(t) = \vec{F}_0 \sin(\omega t + \varphi) \sin^2(\frac{\pi t}{\tau}) & \text{when } t \in [0, \tau], \\ \vec{F}(t) = \vec{0} & \text{elsewhere,} \end{cases} \tag{5}$$

where τ is the total duration of the pulse. The laser electric field is derived from a vector-potential $\vec{A}(t)$, which may be written as

$$\vec{A}(t) = \vec{A}(t_0) - \int_{t_0}^{t} \mathrm{d}t' \vec{F}(t'). \tag{6}$$

In the Schrödinger picture, the transition amplitude from the state i at $t = 0$ to the final state f at $t = \tau$ may be approximated by the *prior* form of the following the variational expression [13]:

$$a_{\mathrm{fi}}^{-} = \lim_{t\to 0} \langle \chi_{\mathrm{f}}^{-}(t) | \chi_{\mathrm{i}}^{+}(t) \rangle - \mathrm{i} \int_0^{\tau} \mathrm{d}t \langle \chi_{\mathrm{f}}^{-}(t) \left| H - \mathrm{i} \overleftarrow{\frac{\partial}{\partial t}} \right| \chi_{\mathrm{i}}^{+}(t) \rangle, \tag{7}$$

where the arrow on the left-hand side indicates the state on which the non-hermitian operator applies, $\chi_{\mathrm{f}}^{-}(\vec{r}, t)$ and $\chi_{\mathrm{i}}^{+}(\vec{r}, t)$ are trial functions to the exact solutions of Eq. (1), subject to the asymptotic conditions

$$\chi_{\mathrm{f}}^{-}(\vec{r}, t) \underset{t\to\tau}{\to} \phi_{\mathrm{f}}^{-}(\vec{r}, t), \tag{8a}$$

$$\chi_{\mathrm{i}}^{+}(\vec{r}, t) \underset{t\to 0}{\to} \phi_{\mathrm{i}}(\vec{r}, t). \tag{8b}$$

Expression (7) provides exact transition amplitudes when one of the two trial functions are exact solutions of (3). The Coulomb–Volkov wave function [14,8] is used as the trial wave function $\chi_{\mathrm{f}}^{-}(\vec{r}, t)$,

$$\begin{cases} \chi_{\mathrm{f}}^{-}(\vec{r}, t) = \phi_{\mathrm{f}}^{-}(\vec{r}, t) L^{-}(\vec{r}, t), \\ L^{-}(\vec{r}, t) = \exp\{\mathrm{i}\vec{A}^{-}(t)\vec{r} - \mathrm{i}\vec{k} \cdot \int_{\tau}^{t} \mathrm{d}t' \vec{A}^{-}(t') \\ \qquad - \frac{\mathrm{i}}{2} \int_{\tau}^{t} \mathrm{d}t \vec{A}^{-2}(t')\}, \end{cases} \tag{9}$$

where $\vec{A}^{-}(t)$ is the variation of $\vec{A}(t)$ over the time interval $[\tau, t]$, i.e.

$$\vec{A}^{-}(t) = -\int_{\tau}^{t} \vec{F}(t) \mathrm{d}t. \tag{10}$$

After an easy algebra using (9) and (10), the expression (7) may be transformed into

$$a_{\mathrm{fi}}^{-} = \int_0^{\tau} \mathrm{d}t \exp\left\{ \mathrm{i}\frac{k^2}{2} t + \mathrm{i}\vec{k} \cdot \int_{\tau}^{t} \mathrm{d}t' \vec{A}^{-}(t') + \frac{\mathrm{i}}{2} \int_{\tau}^{t} \mathrm{d}t' \vec{A}^{-2}(t') \right\} \times \int \mathrm{d}\vec{r} \chi_{\mathrm{i}}^{+}(\vec{r}, t) \exp[-\mathrm{i}\vec{A}^{-}(t) \cdot \vec{r}] \vec{A}^{-}(t) \cdot [\mathrm{i}\vec{k} + \vec{\nabla}] \varphi_{\mathrm{f}}^{-*}(\vec{r}). \tag{11}$$

For a realistic laser pulse, the first term in (7) is zero because both, $\vec{A}^{-}(0) = \vec{0}$ (no direct electric field), and $\phi_{\mathrm{i}}(\vec{r}, t)$ and $\phi_{\mathrm{f}}^{-}(\vec{r}, t)$ are orthogonal.

The choice of the trial wave function $\chi_{\mathrm{i}}^{+}(\vec{r}, t)$ in expression (11) is still open. It should account for most of the bound state part of the exact wave function of a given problem. For instance, when both conditions verify, the photon energy is greater than or equal to the ionization potential, and the ionization process is not saturated, it looks reasonable to replace $\chi_{\mathrm{i}}^{+}(\vec{r}, t)$ by the unperturbed wave function $\phi_{\mathrm{i}}(\vec{r}, t)$. Then, the so-called CV2^{-} approximation is obtained [14]. Electron energy spectra as predicted by CV2^{-} and TDSE have been reported to be in very good agreement for photon energies above the Hydrogen ionization potential $|\varepsilon_{\mathrm{i}}| = 0.5$ [8,11].

On the other hand, for photon energies below the ionization potential secondary peaks appeared in the electron spectrum. These peaks are traced back to population of intermediate states. This may be physically understood by realizing that a short laser pulse has a broad spectrum, thus making possible to populate a wide range of atomic excited states through the absorption of a single photon. It is worth to remark the fact that this intermediate transition may occur even though the laser frequency ω is not in tune.

Hence, improving the theory CV2^{-} implies taking into account a pathway through intermediate bound states. A simple way to do it consists of a different choice for the trial wave function $\chi_{\mathrm{i}}^{+}(\vec{r}, t)$. Since the first Born approximation reproduces very well the non-resonant background of the whole spectrum, even very far from the ionization threshold, it is natural to propose

$$\chi_{\mathrm{i}}^{+}(\vec{r}, t) = \sum_j a_{ji}^{\mathrm{B1}}(t) \phi_j(\vec{r}, t), \tag{12}$$

where $a_{ji}^{\mathrm{B1}}(t)$ is the first Born approximation transition amplitude at time t from the initial state i to the intermediate state $j \equiv (n, l, m)$.

In the present work, the case with the laser frequency resonant to the transition $1\mathrm{s} \to 2\mathrm{p}_0$, that is, when $\omega = (1 - 1/n^2)/2$ (a.u.), is analyzed. The laser intensities are beyond the perturbative condition. Under this situation, the bound state part of the wave function is better described if we restrict to the two-state problem though solving the time-dependent Schrödinger equation in a non-perturbative way. It states as

$$\chi_{\mathrm{i}}^{+}(\vec{r}, t) = a_{1\mathrm{s}}^{\mathrm{TDSE}}(t) \phi_{1\mathrm{s}}(\vec{r}, t) + a_{2\mathrm{p}_0}^{\mathrm{TDSE}}(t) \phi_{2\mathrm{p}_0}(\vec{r}, t), \tag{13}$$

where $a_{1\mathrm{s}}^{\mathrm{TDSE}}(t)$ and $a_{2\mathrm{p}_0}^{\mathrm{TDSE}}(t)$ are the elastic and the excitation amplitude, respectively. They are obtained by solving the TDSE restricted to the two resonantly coupled 1s and $2\mathrm{p}_0$ states. The transition amplitude for the Coulomb–Volkov two-state theory CV-TS is obtained by replacing (13) in (11)

$$\begin{aligned} a_{\mathrm{fi}}^{\text{CV-TS}} = & \int_0^{\tau} \mathrm{d}t a_{1\mathrm{s}}^{\mathrm{TDSE}}(t) \\ & \times \exp\left\{ \mathrm{i}\left(\frac{k^2}{2} - \varepsilon_{1\mathrm{s}}\right) t + \mathrm{i}\vec{k} \cdot \int_{\tau}^{t} \mathrm{d}t' \vec{A}^{-}(t') + \frac{\mathrm{i}}{2} \int_{\tau}^{t} \mathrm{d}t' \vec{A}^{-2}(t') \right\} \\ & \times \vec{A}^{-}(t) \cdot \int \mathrm{d}\vec{r} \varphi_j(\vec{r}) \exp[-\mathrm{i}\vec{A}^{-}(t) \cdot \vec{r}] \vec{A}^{-}(t) \cdot [\mathrm{i}\vec{k} + \vec{\nabla}] \varphi_{\mathrm{f}}^{-*} r \\ & + \int_0^{\tau} \mathrm{d}t a_{2\mathrm{p}_0}^{\mathrm{TDSE}}(t) \\ & \times \exp\left\{ \mathrm{i}\left(\frac{k^2}{2} - \varepsilon_{2\mathrm{p}}\right) t + \mathrm{i}\vec{k} \cdot \int_{\tau}^{t} \mathrm{d}t' \vec{A}^{-}(t') \frac{\mathrm{i}}{2} \int_{\tau}^{t} \mathrm{d}t' \vec{A}^{-2}(t') \right\} \\ & \times \vec{A}^{-}(t) \cdot \int \mathrm{d}\vec{r} \varphi_j(\vec{r}) \exp[-\mathrm{i}\vec{A}^{-}(t) \cdot \vec{r}] \vec{A}^{-}(t) \cdot [\mathrm{i}\vec{k} + \vec{\nabla}] \varphi_{\mathrm{f}}^{-*}(\vec{r}). \end{aligned} \tag{14}$$

The first term accounts for the usual ATI peaks from the 1s initial state [14], while the second term represents a kind of $CV2^-$ amplitude for transitions from the intermediate state $2p_0$. These amplitudes are weighted by the TDSE transition amplitudes in (13) at any time during the laser pulse. The meaning of CV-TS amplitude is quite simple: the system proceeds from a multiphoton transition from either the 1s initial state or from the $2p_0$ intermediate resonantly populated state to undergo a transition into a given continuum state.

The integration over the electron coordinate in (13) may be expressed in terms of the well-known bound-continuum form factor. For hydrogen atoms, it is analytical using Nordsieck's integrals [15]. Therefore, just a simple time numerical integration over the pulse length is necessary to evaluate $a_{\mathrm{fi}}^{\mathrm{CV2}^-}$. Then, as usual, the angular distribution of ejected electrons is given by

$$\frac{\partial^2 P_{\mathrm{fi}}}{\partial E_K \partial \Omega_k} = k|a_{\mathrm{fi}}^-|^2, \tag{15}$$

where E_k and Ω_k are the energy of the ejected electron and the direction of its impulse $\vec{k}$, respectively. Integrating over Ω_k provides the energy distribution $\frac{\partial P_{\mathrm{fi}}}{\partial E_K}$. A further integration over E_k yields the total ionization probability P_{ion}.

3. Application of CV-TS to the ionization of positronium

In this section, the ionization of positronium in its ground state by a laser pulse with photon energy resonant with the first excited state is addressed. Fig. 1 shows a comparison between full numerical solution of the TDSE [11], the $MCV2^-$ perturbative theory [8] and the present CV-TS approximation. The perturbation regime by fixing the laser field amplitude at $F_0 = 0.0025$ a.u. corresponding to an irradiance $I_0 = 2.2 \times 10^{11}$ W/cm^2 is considered. The other parameters of the laser pulse are a frequency $\omega = 0.1875$ and a pulse duration $\tau = 1340.4$ a.u. ($\simeq$32.5 fs) corresponding to 40 laser cycles comparable to the pulse length of a *given* high-harmonics [16]. This length pulse allows us to get well separated ATI peaks. Further, the value of ω does not reach to ionize Ps (1s) with the absorption of a single photon. Therefore, the first ionization peak located close to $\varepsilon_{\mathrm{f}} = 0.0625$ a.u., corresponds to a two-photon process. The electron energy interval is indeed selected to clearly show up the first two principal peaks. The second ATI peak being located at $\varepsilon_{\mathrm{f}} = 0.15625$ a.u. is also displayed. Note that the ponderomotive potential $I_0/(4\omega^2)$ is negligible. A single photon absorption allows the first excited level ($2p_0$) to be reached in a resonant way. The peaks associated with intermediate bound state excitation followed by one photon absorption should lie close to $\varepsilon_{\mathrm{f}} = (\varepsilon_{2p_0} + \omega)/2 \equiv (\varepsilon_{1s} + 2\omega)/2$, i.e. the two-photon ionization from the initial bound state (2s) match the single photon ionization from the intermediate state ($2p_0$). This intermediate state is reached through a resonant process and requires a non-perturbative calculation such as the two-state model approximation. It is noteworthy that CV-TS (dotted line) reproduces even the finer details of the background while MCV2 shows a larger background oscillation as well as overestimates of the exact TDSE spectrum. It is observed that both ATI peaks are slightly overestimated by the two theories. Notwithstanding, it is interesting to note that the sharp interference depth at about $\varepsilon_{\mathrm{f}} \sim 0.07$ a.u. is well reproduced by CV-TS. This is the interference between the amplitudes for the two mechanism described above: direct two-photon absorption from the initial 1s state, and one photon absorption from the intermediate $2p_0$ state. The only failure of the CV-TS comes from the fact that neither intermediate $3p_0$ nor $4p_0$ are accounted for. So the small secondary peaks observed to the right of the first ATI peak are missed. The latter are well represented by $MCV2^-$ [8]. These states could be incorporated in the theory in a perturbative way; however, we are interested in the main ATI peaks behavior when the laser amplitude (irradiance) increases.

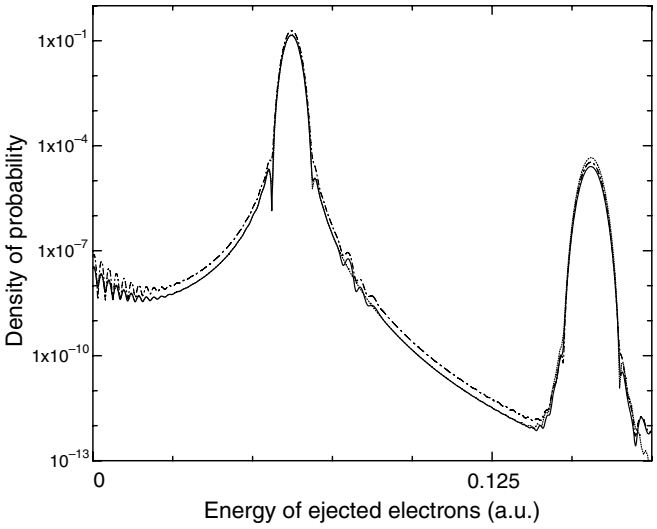

Fig. 1. Ionization of Ps (1s): distribution of ejected electrons (density of probability per energy range) as a function of the electron energy for a laser field amplitude $F_0 = 0.0025$ a.u. ($I_0 = 2.2 \times 10^{11}$ W/cm^2) and a pulse duration of 40 cycles ($\tau = 1340.41$ a.u. $= 32.5$ fs). The photon energy is $\omega = 0.1875$ a.u. Solid line TDSE [8]; dot-dashed line: $MCV2^-$ [8] and dotted line: CV-TS. All quantities are given in atomic units.

Fig. 2 shows our numerical solution for the elastic and transition probabilities of the two-state problem $(1s, 2p_0)$ as a function of time. Three different laser field amplitudes with the same resonant frequency and 80 cycles pulse length are considered. Fig. 2(a)–(c) correspond to $F_0 = 0.0025$ a.u. ($I_0 = 2.2 \times 10^{11}$ W/cm^2), $F_0 = 0.0125$a.u ($I_0 = 5.5 \times 10^{12}$ W/cm^2) and $F_0 = 0.025$ a.u. ($I_0 = 2.2 \times 10^{13}$ W/cm^2), respectively. Rabi oscillations between the 1s and $2p_0$ state populations are observed. The time-dependent Rabi frequency [17] is given by

$$\Omega_{\mathrm{R}}(t) = z_{1s2p} E_0 \sin(\pi t/\tau)^2, \tag{16}$$

where $z_{1s2p} = 1.49$ a.u. is the positronium dipole matrix element. As the laser amplitude increases, Rabi oscillations

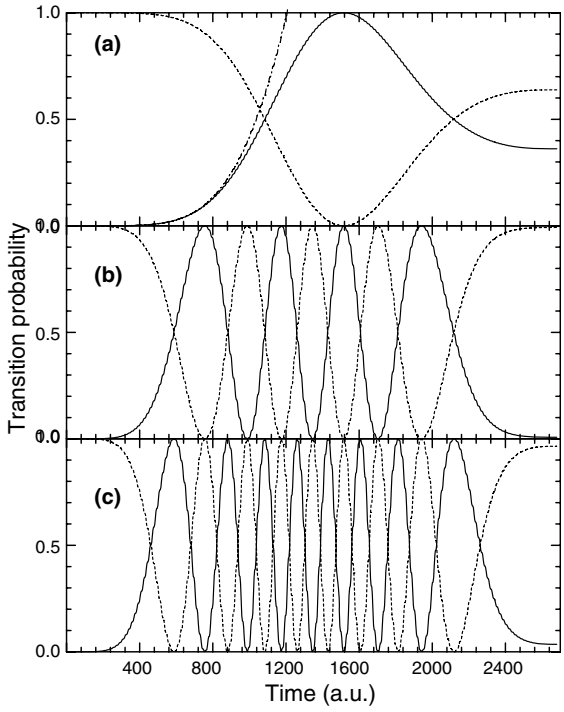

Fig. 2. Transition probability in the two-states model of resonantly coupling of positronium 1s and $2p_0$ by with 80 cycles laser pulse. Solid line: 1s elastic probability, dashed line: $2p_0$ transition probability. (a) $F_0 = 0.0025$ ($I_0 = 2.2 \times 10^{11}$ W/cm^2); dot-dashed line, perturbative $2p_0$ transition probability. (b) $F_0 = 0.0125$ ($I_0 = 5.5 \times 10^{12}$ W/cm^2) and (c) $F_0 = 0.025$ ($I_0 = 2.2 \times 10^{13}$ W/cm^2).

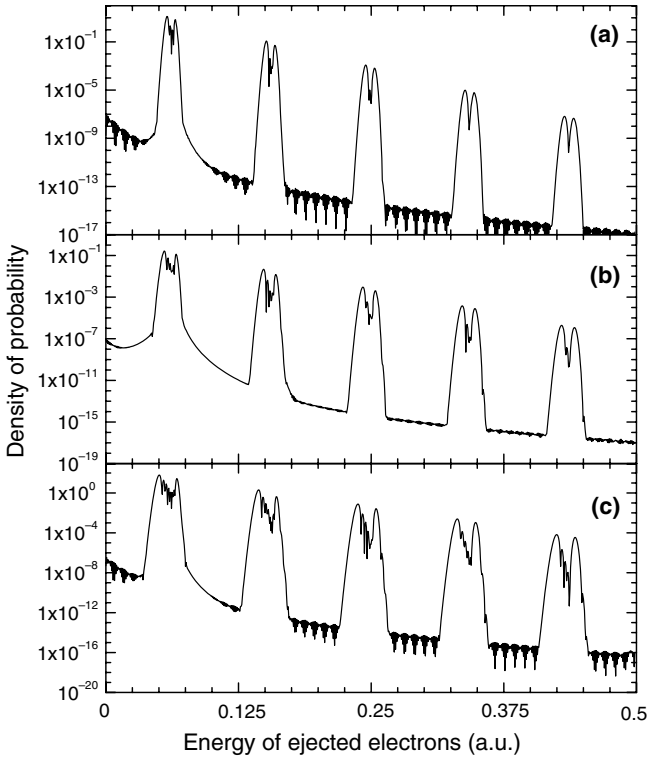

Fig. 3. Ionization of Ps (1s): distribution of ejected electrons (density of probability per energy range) as a function of the electron energy for a pulse duration of 80 cycles ($\tau = 2680.8$ a.u. = 65 fs) and different laser field amplitudes. (a) $F_0 = 0.0125$ a.u. ($I_0 = 5.5 \times 10^{12}$ W/cm^2), (b) $F_0 = 0.0175$ a.u. ($I_0 = 1.07 \times 10^{13}$ W/cm^2) and (c) $F_0 = 0.0025$ a.u. ($I_0 = 2.2 \times 10^{13}$ W/cm^2). All quantities are given in atomic units.

appear in the resonantly coupled state populations. Since the finite pulse duration is featured by a sine-square envelope, Rabi frequency is time dependent with its maximum at the middle of the pulse. Even though the laser amplitude is rather small, the perturbative solution for the $1s \rightarrow 2p_0$ transition probability departs the exact two-state solution around a quarter of the pulse duration, as shown in Fig. 2(a). It may be clearly observed that the frequency around the pulse center in Fig. 2(b) doubles that of Fig. 2(c), as described by the Rabi frequency formulae. Moreover, the oscillation frequency goes to zero at both the beginning and the end of the pulse. Over the main Rabi oscillations there appears a small high frequency correction due to contra rotating term contributions. Corrections due to depopulation of these states are not included. They could be incorporated by a decay rate constant taken into accounts transitions towards the continuum. Work on this line is currently under progress.

In Fig. 3, the CV-TS theoretical electron spectrum of positronium ionization for three different laser field amplitudes $F_0 = 0.0125$, 0.0175 and 0.25 a.u. ($I_0 = 5.5 \times 10^{12}$, 1.07×10^{13} and 2.2×10^{13} W/cm^2) are shown. The pulse duration is fixed to 80 cycles and the resonant $1s \rightarrow 2p_0$ condition is kept. The energy range displayed allows for the observation of up to five ATI broad peaks. However, the normal behavior of the ATI peaks around the maximum is replaced by a structure showing clearly two subpeaks. Notably, this substructure still remains at the five main ATI peaks. The energy splitting of each peak equals to half the Rabi frequency at the middle of the pulse and increases linearly with the field amplitude, doubling between Fig. 3(a) and (c).

As the field amplitude increases, the main ATI structure shifts towards greater electron energies and becomes slightly broader. The small shift is ascribed to increasing ponderomotive potential.

In order to explain the energy splitting of the ATI peaks, the TDSE amplitudes $a_{1s}^{TDSE}(t)$ and $a_{2p_0}^{TDSE}(t)$ in Eq. (14) are approximated by using the rotating wave approximation RWA:

$$a_{1s}^{TDSE}(t) \sim \cos(\Omega_R(t)t/2) = (e^{i\Omega_R(t)t/2} + e^{-i\Omega_R(t)t/2})/2,$$
$$a_{2p_0}^{TDSE}(t) \sim i\sin(\Omega_R(t)t/2) = (e^{i\Omega_R(t)t/2} - e^{-i\Omega_R(t)t/2})/2, \quad (17)$$

where $\Omega_R(t)$ changes slowly with time as given by expression (16). Temporal dependence in (17) may be interpreted as a splitting of both 1s and $2p_0$ energy level in $\mp\Omega_R(t)/2$ a.u., respectively. By replacing (17) in (14), the first term in (14), will contribute to the transition amplitude as coming from two different energy levels $\varepsilon_{1s}^{\mp} = \varepsilon_{1s} \mp \Omega_R(t)/2$, while the second term does represent transitions from the two energy levels $\varepsilon_{2p_0}^{\mp} = \varepsilon_{2p_0} \mp \Omega_R(t)/2$. Therefore, N-photon ionization from $\varepsilon_{1s}^{\mp}$ contributes to the same final

electron–positron relative energy in the continuum as $(N-1)$-photon ionization from $\varepsilon_{2p_0}^{\mp}$: $\varepsilon_{f,N}^{\mp} = N\omega + \varepsilon_{1s}^{\mp} = (N-1)\omega + \varepsilon_{2p_0}^{\mp}$. Actual emitted electron energy peaks are located at $\frac{\varepsilon_{f,N^-}}{2}$ and $\frac{\varepsilon_{f,N^+}}{2}$, the left and the right sub-peaks position, respectively, as shown in Fig. 3. The Rabi frequency time dependence is at the origin of the multi-peak structure between the sub-peaks in Fig. 3(b) and (c). However, Rabi frequency is close to its maximum value $\Omega_R = z_{1s2p}E_0$ most of the time, which explains the location of the two sub-peaks. The sub-peaks energy location average corresponds to the standard multiphoton peak energy location $\bar{\varepsilon}_{f,N} = N\omega + \varepsilon_{1s}$. The asymmetry between the left sub-peak and the right sub-peak are easy to understand inasmuch as the bound-continuum form factor in (14) decreases with the electron continuum energy. Two series multiphoton energy levels are populated starting in each shifted level $\varepsilon_{1s}^{\mp}$. Therefore, the repetitive structure is properly explained. In each case, the multiphoton structure is guarantee by the Coulomb–Volkov final state [14].

It is remarked that the main features concerning the electron spectrum have been understood by using the present quasi-analytical theory. In this sense, the work in reference [10] involving only TDSE results is well complemented by the present study. Furtherly, we have dealt with positronium targets instead of hydrogen considered in [9,10].

4. Conclusions and outlook

We have shown that substituting the genuine initial state by a new *bound* state, which corresponds to the evolution of resonantly coupled 2s and $2p_0$ positronium states in the laser field, explains the Rabi splitting of above threshold ionization peaks. The new bound state takes into account the possibility of building transient intermediate $2p_0$ bound state all along with the laser pulse. Consequently, the multiphoton ionization process occurs from this intermediate level resulting in a considerable enhancement of the ionization probability density. In the proposed theory CV-TS, the initial trial wave function is made of the genuine initial state plus the first excited bound intermediate state with coefficients are given, by a solution of the time-dependent Schrödinger equation of the two-states problem.

Finally, it is worth noting that CV-TS is very simple to implement in more complex atomic species, not only in the simplest case of positronium atoms. Let us point out that different types of laser fields are easy to be treated with a Coulomb–Volkov approach in the length gauge. In fact, all field parameters are contained in the vector-potential $\vec{A}(t)$. Therefore, photons having linear, elliptic or circular polarizations, two-color transitions (with coherent or non-coherent beams) may be studied. Then Coulomb–Volkov like approaches open a wide range of short laser pulse interactions applications.

It is hoped that the effect described in this work may be of interest for experimentalist such as the Aarhus group, since the laser frequency required for the experiment with positronium has been reported to be available [3].

Acknowledgements

V.D. Rodríguez acknowledges support by the Universidad de Buenos Aires under grant X259, by the Consejo Nacional de Investigaciones Científicas y Técnicas (CONICET) under PIP 583 and the program ECOS/CONICYT, Grant No. C03E01.

References

[1] L.B. Madsen, P. Lambropoulos, Phys. Rev. A 59 (1999) 4574.
[2] H.A. Bethe, E.E. Salpeter, Quantum Mechanics of One and Two-Electron Atoms, Springer-Verlag, Berlin, 1957.
[3] P. Balling, D. Fregenal, T. Ichioka, H. Knudsen, H.-P.E. Kristiansen, J. Merrison, U.I. Uggerhoj, Nucl. Instr. and Meth. B 221 (2004) 200.
[4] G.F. Gribakin, H. Knudsen, C.M. Surko, Phys. Scripta 70 (2004) C1.
[5] K.P. Ziock et al., Phys. Rev. Lett. 64 (1990) 2366.
[6] L.B. Madsen, L.A.A. Nikolopoulos, P. Lambropulos, Eur. Phys. J. D 10 (2000) 67;
L.B. Madsen, Nucl. Instr. and Meth. B 221 (2004) 174.
[7] B. Henrich, K.Z. Hatsagortsyan, C.H. Keitel, Phys. Rev. Lett. 93 (2004) 013601.
[8] V.D. Rodríguez, E. Cormier, R. Gayet, Phys. Rev. A 69 (2004) 0530402.
[9] F. Faisal, J. Moloney, J. Phys. B 4 (1981) 3603.
[10] K.J. La Gattuta, Phys. Rev. A 47 (1993) 1560.
[11] E. Cormier, P. Lambropoulos, J. Phys. B: At. Mol. Opt. Phys. 30 (1997) 77.
[12] V.P. Krainov, H.R. Reiss, B.M. Smirnov, Radiative Processes in Atomic Physics, John Wiley & Sons Inc., 1997.
[13] Yu.N. Demkov, Variational Principles in the Theory of Collisions, Pergamon Press, Oxford, 1963.
[14] G. Duchateau, E. Cormier, R. Gayet, Phys. Rev. A 66 (2002) 023412.
[15] A. Nordsieck, Phys. Rev. 93 (1954) 785.
[16] A. Bouhal, P. Salières, P. Breger, P. Agostini, G. Hamoniaux, A. Mysyrowicz, A. Antonetti, R. Constantinescu, H.G. Muller, Phys. Rev. A 58 (1998) 389.
[17] I.I. Rabi, Phys. Rev. 51 (1932) 652.